Research
A SCIENCE PARTNER JOURNAL

RESEARCH ARTICLE

Aggregation-Induced Catalysis: Asymmetric Catalysis with Chiral Aggregates

Yao Tang[1†], Yu Wang[2†], Qingkai Yuan[1†], Sai Zhang[1], Jia-Yin Wang[2,3], Shengzhou Jin[2], Ting Xu[2], Junyi Pan[2], Kazimierz Surowiec[1], and Guigen Li[1,2*]

[1]Department of Chemistry and Biochemistry, Texas Tech University, Lubbock, TX 79409-1061, USA. [2]School of Chemistry and Chemical Engineering, Nanjing University, Nanjing 210093, China. [3]School of Pharmacy, Continuous Flow Engineering Laboratory of National Petroleum and Chemical Industry, Changzhou University, Changzhou, Jiangsu 213164, China.

*Address correspondence to: guigen.li@ttu.edu
†These authors contributed equally to this work.

Citation: Tang Y, Wang Y, Yuan Q, Zhang S, Wang JY, Jin S, Xu T, Pan J, Surowiec K, Li G. Aggregation-Induced Catalysis: Asymmetric Catalysis with Chiral Aggregates. *Research* 2023;6:Article 0163. https://doi.org/10.34133/research.0163

Submitted 28 January 2023
Accepted 17 May 2023
Published 9 June 2023

Copyright © 2023 Yao Tang et al. Exclusive licensee Science and Technology Review Publishing House. No claim to original U.S. Government Works. Distributed under a Creative Commons Attribution License 4.0 (CC BY 4.0).

So far, there have been 4 methods to control chirality including the use of chiral auxiliaries, reagents, solvents, and catalysts documented in literature and textbooks. Among them, asymmetric catalysts are normally divided into homogeneous and heterogeneous catalysis. In this report, we present a new type of asymmetric control—asymmetric catalysis via chiral aggregates that would not belong to the above categories. This new strategy is represented by catalytic asymmetric dihydroxylation reaction of olefins in which chiral ligands are aggregated by taking advantage of typical aggregation-induced emission systems containing tetrahydrofuran and H_2O cosolvents. It was proven that the chiral induction can be enhanced from er of 78:22 to 97:3 simply by changing the ratios of these 2 cosolvents. The formation of chiral aggregates of asymmetric dihydroxylation ligands, $(DHQD)_2PHAL$ and $(DHQ)_2PHAL$, has been proven by aggregation-induced emission and a new analytical tool—aggregation-induced polarization established by our laboratory. In the meanwhile, chiral aggregates were found to be formed either by adding NaCl into tetrahydrofuran/H_2O systems or by increasing concentrations of chiral ligands. The present strategy also showed promising reverse control of enantioselectivity in the Diels–Alder reaction. This work is anticipated to be extended broadly to general catalysis, especially to asymmetric catalysis in the future.

Introduction

Over the past half a century, asymmetric synthesis and catalysis have been actively pursued in chemical and materials sciences [1–4]. Increasing numbers of drugs and pesticides contain chiral structural units in their structures since drug actions require conformational matching to increase their potency and selectivity toward receptors and other active targets inside and on the surfaces of cells [5–9]. Structural design of pharmaceuticals plays key role in reducing or avoiding severe side effects during their action processes [6]. In the meanwhile, more advanced materials, especially nano- and photoelectronic materials contain micro- and macrochiral units requiring various levels of asymmetric factors [10–16]. Therefore, the control of chirality will continue to play a crucial role in the aforementioned fields. So far, 4 synthetic strategies have been developed for controlling molecular chirality relying on the use of chiral catalysts (bio- and chemocatalysts), chiral auxiliaries, chiral reagents, and chiral solvents [17–27]. There have been no other asymmetric controllers beyond these 4 methods documented in literature so far.

Very recently, our laboratories have developed a new tool, stoichiometric aggregation-induced asymmetric synthesis (AIAS), providing asymmetric access to chiral amino products by taking advantage of chiral aggregates of group-assisted purification reagents, *N*-phosphonyl imines (Fig. 1) [28–30]. The asymmetric group-assisted purification synthesis of functionalized 2,3-dihydrobenzofurans by reacting salicyl *N*-phosphonyl imines with dialkyl bromomalonates was conducted in various typical cosolvent systems of aggregation [28]. By changing the ratios of cosolvents of tetrahydrofuran (THF) and ethanol, the chiral products were controlled toward different directions, i.e., (*R*)-isomeric products were predominantly formed over (*S*)-counterparts when amounts of ethanol were increased, and vice versa. The formation of chiral aggregates was confirmed by aggregation-induced emission (AIE) [31–33] and, concurrently, by a new analytical tool—aggregation-induced polarization (AIP), which was established by our laboratory [28,34–35]. This work would change the traditional thoughts on organic synthesis in which individual molecules of starting materials are involved for forming products, i.e., organic reactions and synthesis are about the behaviors of freely distributed single molecules in solutions. The concentrations of reactants are based on the above stoichiometric calculations. However, the AIAS work proved that organic reactions would involve a combination of individual molecules, their dimers, trimers,

etc., instead of only individual molecules in reaction systems. In particular, the reactions would consist of a series of chiral aggregates, which can increase the enantioselective control of asymmetric reactions, and even direct reactions toward different directions asymmetrically. The formations of achiral aggregates (for normal reactions) and chiral aggregates (for asymmetric reactions) during reaction processes would depend on various factors, such as concentrations, solvents/cosolvents, temperature, additives, pressure, etc. The opposite control provides a unique tool to control the chirality of organic and medicinal building blocks without changing the chirality of starting materials and catalysts. Therefore, this work belongs to greener and more environmentally friendly synthesis and production. By simply changing inexpensive solvents, stereoselectivity enhancement and opposite stereoisomers can be conveniently achieved. The latter avoids the tedious preparation of starting materials of opposite chirality and minimizes manpower, energy usage, and waste generation.

Inspired by our previous work on stoichiometric AIAS, our next effort is to establish asymmetric catalysis by taking advantage of chiral aggregates. One of the most successful asymmetric catalytic reactions, asymmetric dihydroxylation (AD) of alkenes, was thus selected for this purpose. In this report, we would like to disclose our preliminary results of this investigation by conducting AD under a series of new aggregation conditions.

Results

Rationale and synthesis

We began this work using one of the most influential asymmetric catalytic reactions—the Sharpless catalytic AD reaction owing to its simplicity with predictable asymmetric control by well-known and commercially available chiral ligands [36–38]. The commercial AD mixes containing the ligands $(DHQ)_2PHAL$ and $(DHQD)_2PHAL$, referred to as AD-mix-α and AD-mix-β, respectively, were directly used for the reaction at room temperature. For the sake of aggregation, the cosolvents of THF–H_2O commonly adopted in AIE [31–33] and AIP [34–35] were used for the present study instead of the traditional AD solvents of acetone, acetonitrile, and alcohols together with water. Among many AD substrates, styrene and its derivatives were considered since they are best researched mechanistically in AD due to their simplicity.

The reactions were carried out in vials equipped with magnetic stirrers and 2.0 or 6.0 ml of cosolvents, as described in the literature [38]. Styrene (0.20 or 0.60 mmol) and AD-mix-α or AD-mix-β (0.28 or 0.84 g) were added to each vial. The resulting mixtures were stirred at room temperature for 24 h until starting materials were consumed, as revealed by thin-layer chromatography. The reactions were quenched by adding sodium sulfite and then stirred at room temperature for 1 h. The resulting mixtures were then extracted several times with ethyl acetate. The organic layers were combined, dried over anhydrous Na_2SO_4, and concentrated to give a mixture of a crude diol containing chiral ligand, which was subsequently purified through flash chromatography prior to chiral high-performance liquid chromatography (HPLC) analysis.

The relationship between solvent ratios and enantioselectivity was researched by setting them toward 2 directions with the ratios of THF and H_2O on the *x* horizontal coordinate correlating to enantioselectivity on the *y* vertical ordinate. Following our previous manner, the ratio of v/v = 1:1 was first set in the middle for various reactions to obtain average data as the reference on the *x* horizontal coordinate. The reaction was performed in 9 sets of cosolvents consisting of THF/ H_2O: 4.5:1, 3:1, 1.5:1, 1:1, 1:1.5, 1:3, 1:4.5, and 1:6 (Fig. 1 and Table 1).

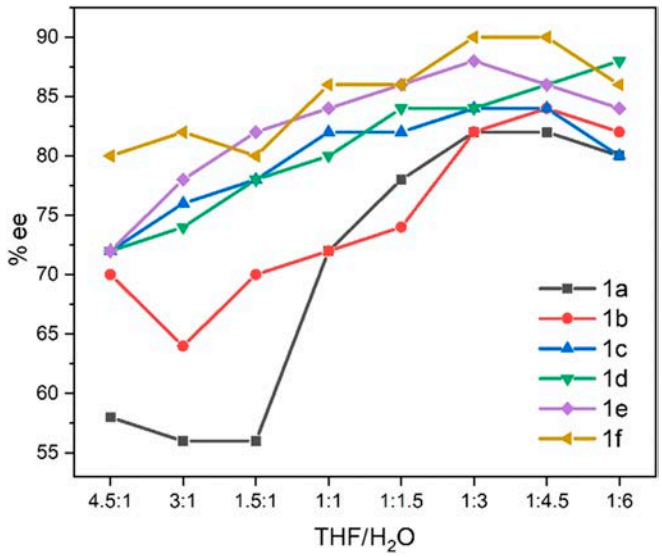
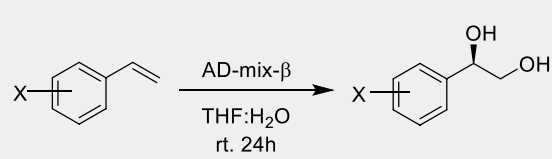


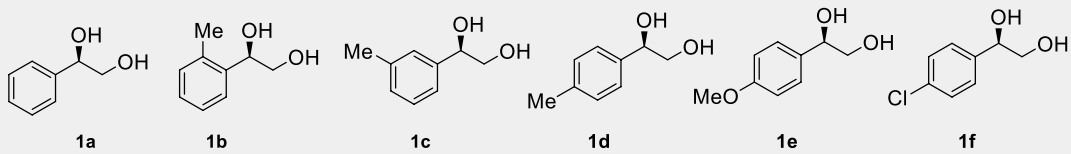
Fig. 1. Curve description of er enhancement in aggregation-induced catalysis from AD-mix-β.

To avoid or minimize possible variations of experimental skills, especially purifications of column chromatography, we determined the yield of each trail by crude proton nuclear magnetic resonance (NMR) spectroscopic analysis using CH_2Br_2 as the internal standard. As described in Table 1, each trial of styrene-**1a** produced a high yield that was nearly unaffected by the ratios of solvents. For the case of styrene-**1b**, enantioselectivity is slightly higher than that of styrene-**1a**, albeit yields drop ~10% as compared with the latter. This observation would be attributed to the bigger steric effect by *o*-Me group on the phenyl ring when the ligand–metal complex approaches this substrate. Cases of styrene-**1c** and -**1d** showed similar enantioselectivity and yields, except for the first trial of **1c**, giving a lower yield. As the fraction of H_2O was increased as the major solvent in the cosolvent systems, enantioselectivity was increased in the above cases in general. For the case of styrene-**1e** attached by a strong electron-donating group (*p*-OMe), chemical yields dropped again, but enantioselectivity was gradually increased as *fw* became bigger. A similar trend was observed for styrene-**1f** in regard to enantioselectivity, but chemical yields were substantially diminished to a range from 45% to 58%.

More specifically, for case **1a**, the largest jump of er occurred from S:R = 78:22 to 86:14 when v-THF/v-H_2O was increased from 1.5:1 to 1:1, which eventually reached 91:9 when the v-THF/v-H_2O ratio was set within a range of 1:3 to 1:6 as shown in both Table 1 and Fig. 1. For case **1b**, there is not an obvious er jump depicted, but a steady er enhancement was observed as H_2O became more predominant in the reaction mixture within the whole range of v-THF/v-H_2O ratios. A similar situation occurred for the rest of other cases, **1c** to **1f**, although er dropped a little for most of these cases when the v-THF/v-H_2O ratio reached 1:6. The present phenomenon would be attributed to the aggregate formation from $(DHQD)_2PHAL$-based catalyst species, the higher the *fw* of cosolvents, the more aggregation for the asymmetric catalysis. It seems that electronic effects of

Table 1. Primary results of aggregation-induced catalytic AD reaction.[a]





1a 1b 1c 1d 1e 1f

Entry THF/H_2O	1a		1b		1c		1d		1e		1f[b]	
	R:S	Yield[c]	R:S[d]	Yield	R:S	Yield	R:S	Yield	R:S	Yield	R:S	Yield
4.5:1	**79**:21	99%	**85**:15	82%	**86**:14	68%	**86**:14	99%	**86**:14	78%	**90**:10	45%
3:1	**78**:22	99%	**82**:18	82%	**88**:12	98%	**87**:13	99%	**89**:11	78%	**91**:9	53%
1.5:1	**78**:22	99%	**85**:15	84%	**89**:11	99%	**89**:11	99%	**91**:9	84%	**90**:10	54%
1:1	**86**:14	99%	**86**:14	85%	**91**:9	94%	**90**:10	99%	**92**:8	84%	**93**:7	50%
1:1.5	**89**:11	99%	**87**:13	80%	**91**:9	94%	**92**:8	99%	**93**:7	86%	**93**:7	48%
1:3	**91**:9	99%	**91**:9	86%	**92**:8	99%	**92**:8	99%	**94**:6	88%	**95**:5	50%
1:4.5	**91**:9	99%	**92**:8	80%	**92**:8	99%	**93**:7	99%	**93**:7	86%	**95**:5	50%
1:6	**90**:10	97%	**91**:9	84%	**90**:10	95%	**94**:6	99%	**92**:8	84%	**93**:7	58%

[a]Standard condition: Styrene (0.2 mmol) and 0.28 g of AD-mix-β in 2 ml of THF/H_2O mixture at room temperature for 24 h.

[b]Condition: Styrene (0.6 mmol) and 0.84 g of AD-mix-β in 6 ml of THF/H_2O mixture at room temperature for 24 h.

[c]All yields determined by crude ^{1}H NMR with internal standard.

[d]All R:S ratios determined by HPLC analysis of isolated samples.

styrene substrates did not show obvious effects on er enhancement trend when substitutes of Me, OMe, and Cl were attached to the phenyl ring, although electron-withdrawing Cl moiety led to low chemical yields than in other cases.

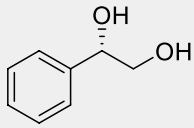
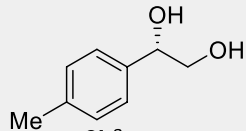
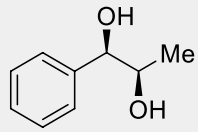
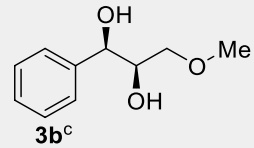
Since $(DHQD)_2PHAL$ and $(DHQ)_2PHAL$ are not exactly defined as enantiomers considering Et attachment on C(sp^3) chiral centers on their tricyclic frames, AD-mix-α was next examined for the present aggregation-induced asymmetric catalysis. Two representative substrates, styrene, and 4-Me–styrene were selected for this purpose. As described in Table 2 and Fig. 2, both cases showed steady enantioselectivity enhancement as H_2O became more predominant in the AD reaction mixture within the whole range of v-THF/v-H_2O ratios, affording er from R:S = 18:82 to 12:88 and 16:84 to 7:93, respectively. However, er dropped back a little in the case of **2a** after the v-THF/v-H_2O ratio turned from 1:3. Both **1a** and **1b** cases afforded consistent chemical yields from 81% to 89% and 90% to 96%, respectively, within the whole range of v-THF/v-H_2O ratios.

The present aggregation-induced asymmetric catalysis was also proven to be effective for *trans*-β-substituted styrenes, which were examined under the standard AD condition. As revealed in Table 2 and Fig. 2, the ee values in **3a** case with methyl substitution on β position boosted from 78% to 94% from the ratio of v-THF/v-H_2O = 6:1 to 1:3, but as the proportion of water in the combination was increased, the ee value decreased somewhat to 88%. Notably, the **3n**-diol with a methyl ester on the β position of styrene can only give 70% ee with a cosolvent ratio of 6:1 (v-THF/v-H_2O). However, as the proportion of water in the solvent system grew, the ee value reached as high as 94% and dropped slightly to 92% when the ratio hit 1:6 (v-THF/v-H_2O).

Aggregation investigation on chiral ligands—AIE and AIP

To confirm the existence of the aggregates from chiral quinine ligands during the catalytic pathway, we investigated the aggregation of $(DHQD)_2PHAL$ and $(DHQ)_2PHAL$ via ultraviolet-visible (UV-vis) spectroscopy and photoluminescence (PL) spectroscopy. To conduct the UV-vis analysis of $(DHQD)_2PHAL$ and $(DHQ)_2PHAL$, we dissolved 2 chiral ligands in THF at a concentration of c = 25 μg/ml. Two chiral ligands exhibited nearly identical spectral behaviors featuring maximum absorptions at around 290, 320, and 334 nm (Fig. 6A). THF and water, the cosolvents used in the asymmetric catalytic step, were now chosen to study both ligands' AIE properties. Figure 6B and C shows that $(DHQD)_2PHAL$ and $(DHQ)_2PHAL$ exhibited aggregation phenomena by adjusting the irradiation power to 700 V and excitation wavelengths to 350 nm. Moreover, these 2 ligands demonstrated a similar AIE property, as their emission intensity grew progressively from 50 to 400 when the water fraction was changed from 0% to 50%. Interestingly, the emission

Table 2. Aggregation-induced catalytic AD based on $(DHQ)_2PHAL$ (2a and 2b) and on *trans*-styrene (3a and 3b).

	 **2a**[a]		 **2b**[a]		 **3a**[b]		 **3b**[c]	
THF/H_2O	R:S[d]	Yield[e]	R:S	Yield	RR:SS	Yield	RR:SS	Yield
4.5:1	18:**82**	81%	16:**84**	90%	**89**:11	52%	**89**:11	50%
3:1	18:**82**	86%	15:**85**	95%	**89**:11	72%	**90**:10	88%
1.5:1	15:**85**	86%	13:**87**	93%	**91**:9	73%	**92**:8	93%
1:1	13:**87**	85%	10:**90**	93%	**93**:7	73%	**93**:7	90%
1:1.5	10:**90**	83%	9:**91**	93%	**95**:5	74%	**95**:5	96%
1:3	7:**93**	87%	7:**93**	96%	**97**:3	72%	**97**:3	90%
1:4.5	10:**90**	89%	7:**93**	95%	**95**:5	74%	**97**:3	87%
1:6	12:**88**	89%	7:**93**	96%	**94**:6	70%	**96**:4	87%

[a]Condition: Styrene (0.2 mmol) and 0.28 g of AD-mix-α in 2 ml of THF/H_2O mixture at room temperature for 24 h.

[b]Condition 3a: Styrene (0.6 mmol) and 0.84 g of AD-mix-β in 6 ml of THF/H_2O mixture at room temperature for 24 h.

[c]Condition: Styrene (0.2 mmol) and 0.28 g of AD-mix-β in 2 ml of THF/H_2O mixture at room temperature for 24 h.

[d] All R:S and RR:SS ratios were determined by chiral HPLC analysis of isolated samples.

[e]All yields determined by crude ^1H NMR with internal standard.

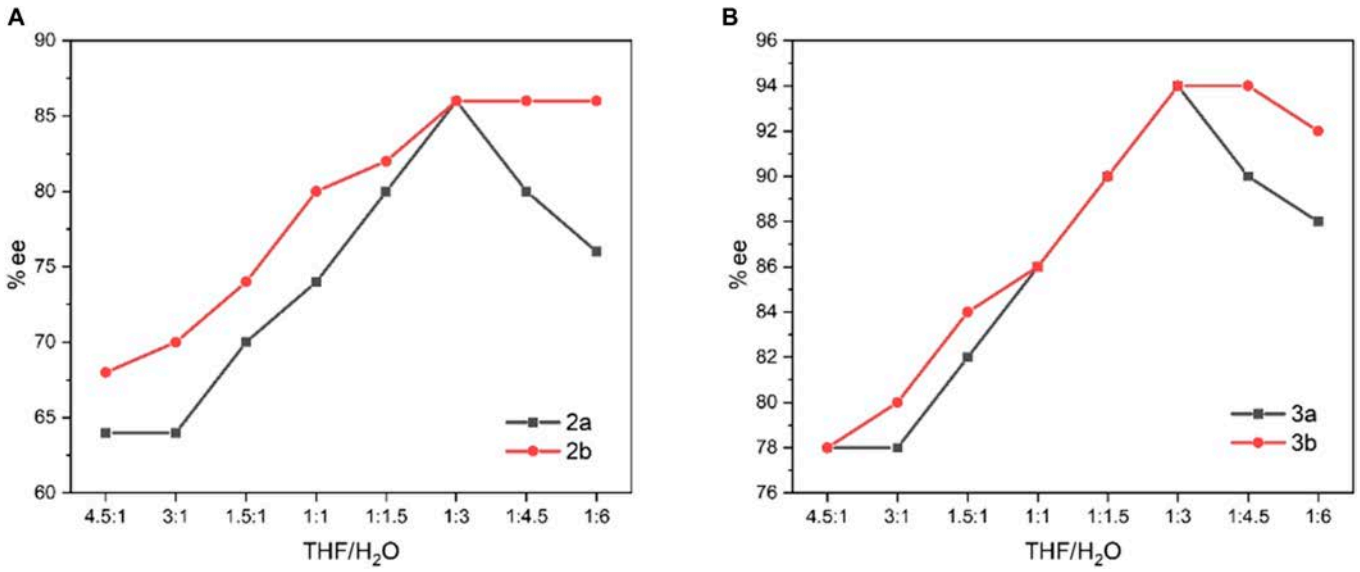


Fig. 2. Curve descriptions of er enhancement in aggregation-induced catalysis via (A) AD-mix-α and (B) *trans*-β-substituted styrenes via AD-mix-β.

maxima of $(DHQD)_2PHAL$ jumped dramatically to around 780 as another 10% water fraction was added. Compared with the $(DHQD)_2PHAL$, the emission maxima of $(DHQ)_2PHAL$ were only raised to about 500.

Next, we investigated whether the polarity of the protonic component in the cosolvent can enhance the fluorescence intensity of chiral ligands. Both ligands with a 50% water fraction were chosen as the model for this experiment, which was inputted the same excitation wavelength and voltage for excitation as that in AIE studies. Figure 6D shows that the PL intensities of $(DHQ)_2PHAL$ were increased slightly as the protonic component became polar. The PL intensities of $(DHQD)_2PHAL$ featured a more robust growth according to the NaCl concentration. As the NaCl concentration in the pure solvent mixture rose to 0.05 g/100 ml, the intensity climbed from 360 to 386. Finally, the intensity reached 403 as the NaCl concentration was doubled. We believe that this observation has a marked potential for AIE enhancement.

Dynamic light scattering (DLS) experiments show that the size of aggregates from AD-β increased with water fraction rising from 5% to 45%, which matched the results of the emission study (Fig. 3). This result also demonstrated that increasing polarity affects the size distribution, increasing from 344 to 1,944 nm. In addition, the largest diameter size of the aggregates jumped from 1,635 to 6,540 nm in the 1:1 THF/water mixture as time went to 2 h, suggesting that the aggregate particles formed gradually (Fig. 4). This result supported that the molecular aggregation was ongoing during the dihydroxylation reaction in favor of enantioselective enhancement.

The aggregation study was further extended by investigating the correlation between the specific optical rotation of chiral ligands'concentrations. As shown in Fig. 5, the specific rotation of $(DHQD)_2PHAL$ surged from −202° to −176° according to the concentration climbed from 0.5 to 2.0 mg/ml and then continuously increased to −179° as the sample was concentrated to 16 mg/ml. On the contrary, the specific rotation of $(DHQ)_2PHAL$ was decreased significantly from 358° to 266° as the concentration was increased from 0.5 to 4.0 mg/ml and, eventually, was remained constant at 263° as the concentration reached 16.0 mg/ml.

The correlation of chiral aggregates to AIP was further explored to render optical rotation enhancement or adjustment as more polar solvent was added in cosolvents [34,35]. AIP measurements of chiral dimeric quinine ligands were conducted using a Rudolph polarimeter (Rudoph Research Analytica APIV/2W) with the sodium lamp emitting light at 589 nm as the light source. The samples were prepared at a consistent concentration ($c = 2$ mg/ml) in the cosolvents commonly used AIE and, for the present AD, were thus utilized. The average specific rotation values taken from 3 measurements were considered the most authentic results and further plotted to relation curves with specific rotation on the *y* axis. The water fraction was set at the component of 5% (v/v) on the *x* horizontal axis. As shown in Fig. 6E and F, $(DHQD)_2PHAL$ demonstrated a substantial increase trend in the specific optical rotation values with gradually increased water fractions, from −186.5° to −132.5° during the water fraction's changing from 0% to 65%. In contrast, $(DHQ)_2PHAL$ showed an opposite trend, which featured a consistent descending trend, in which the optical rotation value dramatically fell from 292.5° to 250°.

Last but not least, the present aggregation-induced asymmetric catalysis strategy demonstrated promising results on other reactions. For example, in the same cosolvent system containing THF and H_2O, organocatalytic asymmetric Diels–Alder reaction between 1,3-diphenylisobenzofuran and (*E*)-but-2-enal depicted opposite enantioselectivity with respect to *endo*-isomer by increasing *fw* values. The exclusive *endo*/*exo* selectivity was observed under this aggregation system that is different from the reported counterpart using the same catalyst of (*S*)-5-benzyl-2,2,3-trimethylimidazolidin-4-one (Fig. S17) [38–41].

Discussion

In summary, we have established aggregation-induced asymmetric catalysis as a new tool providing access to chiral products. Enantioselectivity enhancement was witnessed by the Sharpless catalytic AD of alkenes by changing the ratios of cosolvents of THF and H_2O. Through the formation of chiral aggregates, the chirality of products can even be reversed, which is extremely challenging for classical tools to achieve. The formation of chiral aggregates has been proven by AIE and, concurrently, by AIP of chiral ligands in typical AIE cosolvent systems. Aggregation was also investigated by changing the concentration of chiral ligands or by adding NaCl into the solution for PL enhancement. Together with our previous stoichiometric AIAS, which afforded more notable opposite control

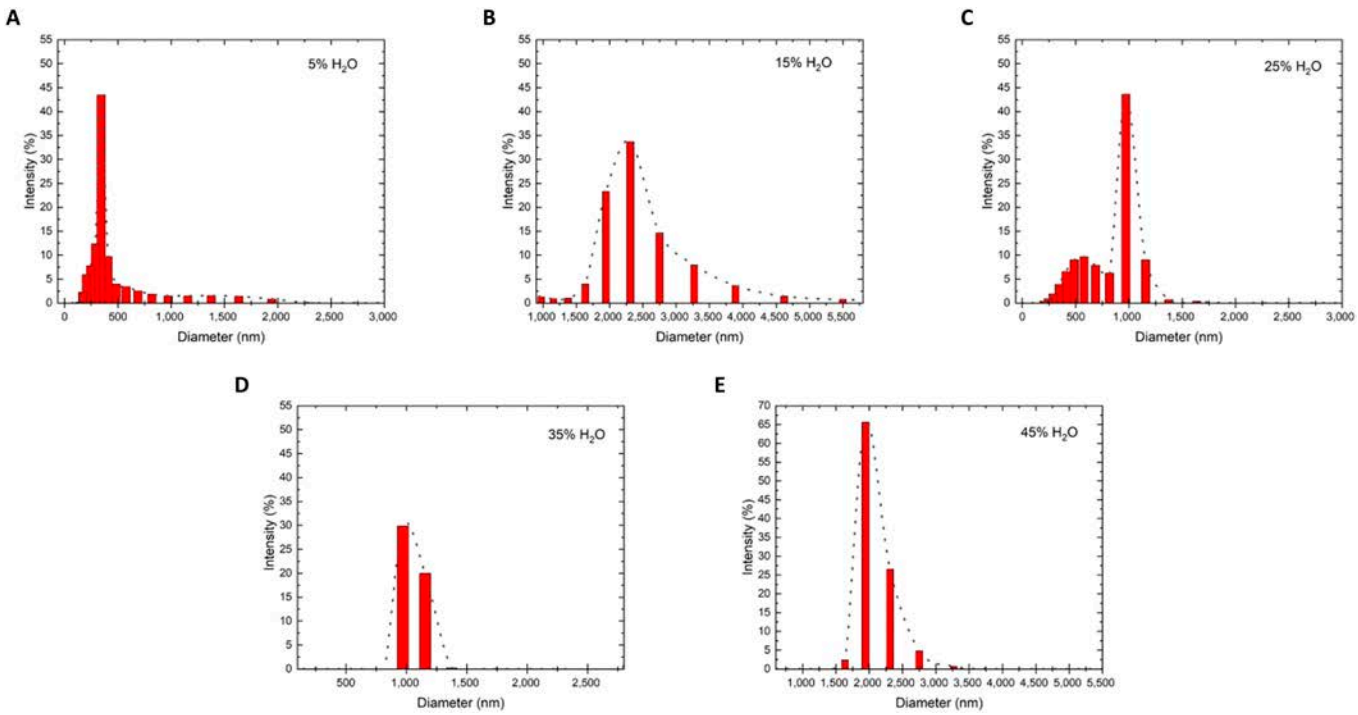


Fig. 3. DLS particle size distribution curves of AD-β obtained in THF/water mixture (5% to 45% H_2O, v/v).

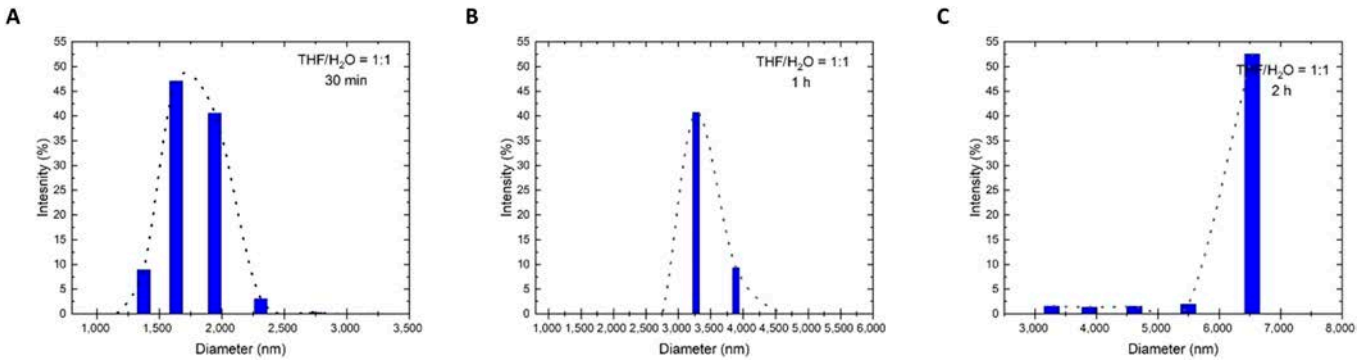


Fig. 4. DLS particle size distribution curves of AD-β obtained in THF/water mixture (1:1 THF/H_2O) at times of 30 min (A), 1 h (B), and 2 h (C).

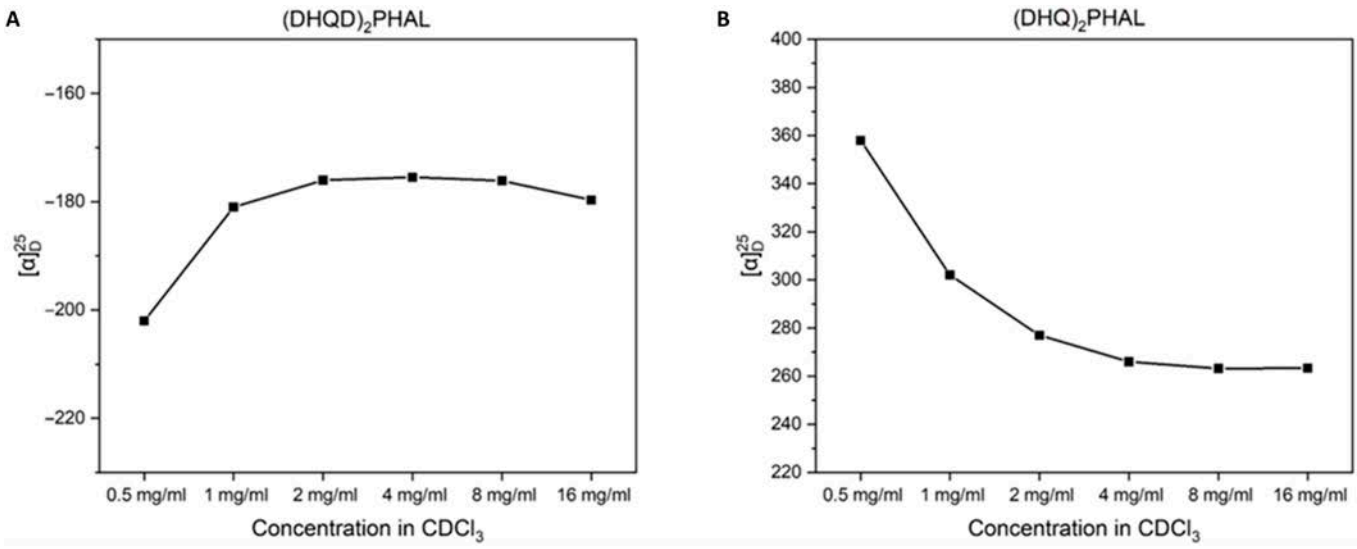


Fig. 5. Correlation between specific optical rotation and sample concentrations.

of chirality simply by changing ratios of THF and H_2O, the present work is anticipated to further find more academic and industrial applications in asymmetric synthesis. We believe that the formation of aggregates from starting materials, intermediates, catalytic species, and products in organic and aqueous media would be quite general, especially when the above 4 categories of aggregates coexist during the reaction processes. This work also indicates that the biological catalysis in water systems via bioaggregates (e.g., enzyme aggregates) would be common and is worth further investigation. It will play an increasingly important role in research on biocatalysis, greener and more environmentally friendly synthesis and materials in the future.

Materials and Methods

Unless otherwise stated, all reactions were magnetically stirred and conducted in oven-dried glassware in anhydrous solvents under Ar, applying standard Schlenk techniques. Solvents and liquid reagents, as well as solutions of solid or liquid reagents, were added via syringes, stainless steel, or polyethylene cannulas through rubber septa or through a weak Ar counterflow. Solvents were removed under reduced pressure at 40 to 65 °C using a rotavapor. All given yields are isolated yields of chromatographically and NMR spectroscopically materials. Internal standard was performed for yield measurements as well. All commercially available chemicals were used as received without further purification. Solvents were obtained as follows: THF is delivered from an Innovation Technology solvent system.

The ^1H and ^{13}C NMR spectra were recorded in $CDCl_3$ or dimethyl sulfoxide (DMSO)–d_6 on 400- and 500-MHz instruments with TMS as internal standard. For referencing of the ^1H NMR spectra, the residual solvent signal ($\delta = 7.26$ for $CDCl_3$ and $\delta = 2.50$ for DMSO-d_6) were used. In the case of the ^{13}C NMR spectra, the signal of solvents ($\delta = 7.16$ for $CDCl_3$ and $\delta = 39.52$ for DMSO-d_6) were used. Chemical shifts (δ) were reported in ppm with respect to TMS. Data are represented as follows: chemical shift, multiplicity (s = singlet, d = doublet, t = triplet, and m = multiplet), coupling constant (J, Hz), and integration. Fluorescence data were collected using the Cary Eclipse Fluorescence Spectrophotometer and Eclipse ADL program. Measurements were performed with diluted samples with 0.1 mM concentrations at 400-nm maximum excitation wavelength under electric power at 900 V. Optical rotations were measured with a Rudolph Research Analytical APIV/2W Polarimeter at the indicated temperature with a sodium lamp. Measurements were performed in a 2-ml tube with the concentration unit of grams per 100 ml in the corresponding solvents. AIP measurements

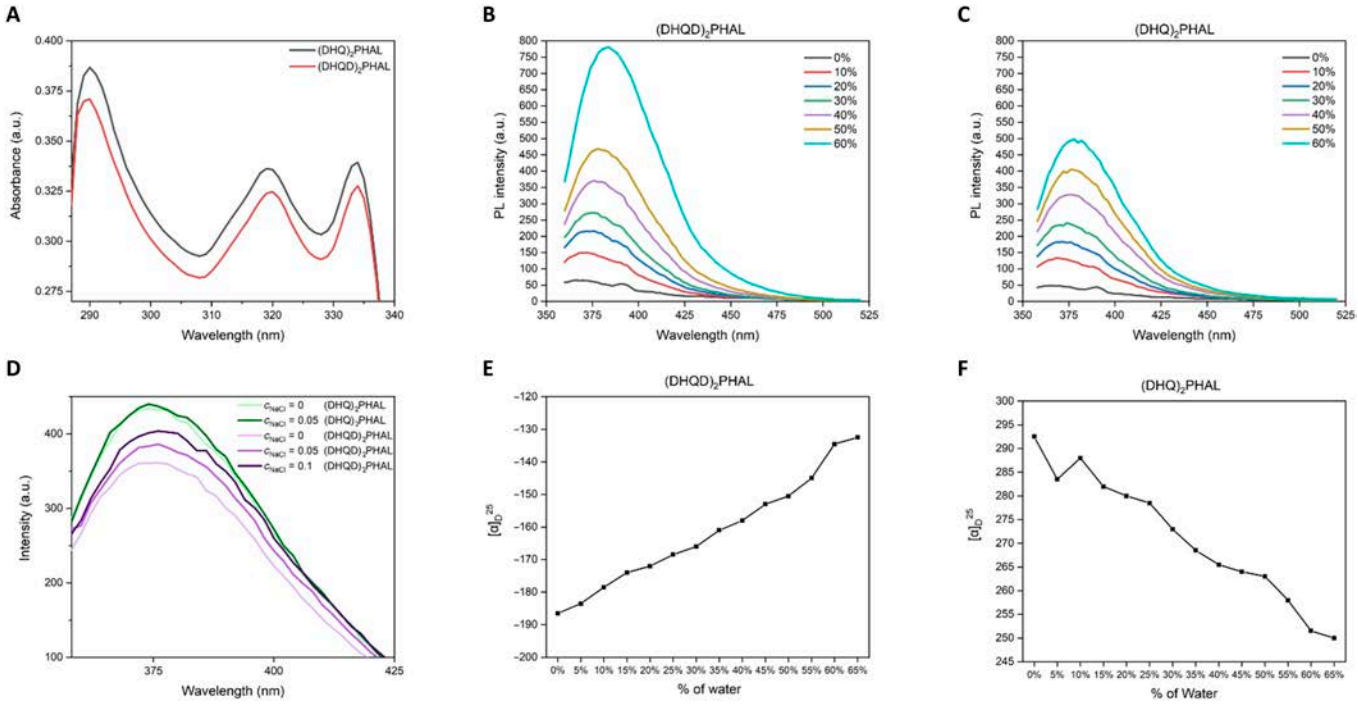


Fig. 6. (A) UV-vis absorption of $(DHQD)_2PHAL$ and $(DHQ)_2PHAL$ in THF; $c = 25$ μg/ml PL spectra of $(DHQD)_2PHAL$ (B) and $(DHQ)_2PHAL$ (C) in THF/water mixtures with different water fractions (*fw*); $c = 0.1$ mM; $\lambda ex = 350$ nm. (D) PL spectra of $(DHQD)_2PHAL$ and $(DHQ)_2PHAL$ in THF/water mixtures at 50% water fraction with different concentrations of NaCl; $c_{chiral\ ligands} = 0.1$ ml, $c_{NaCl} =$ g/100 ml; $\lambda ex = 350$ nm AIP of $(DHQD)_2PHAL$ (E) and $(DHQ)_2PHAL$ (F) in THF/water cosolvents; $c = 2$ mg/ml. a.u., arbitrary units.

of chiral dimeric quinine ligands was conducted using a Rudolph polarimeter (Rudoph Research Analytica APIV/2W) with the sodium lamp emitting light at 589 nm as the light source.

Acknowledgments

We thank A. Cozzolino and O. Villanueva for assistance with the DLS analysis. **Funding:** We would like to acknowledge the financial support from Robert A. Welch Foundation (D-1361-20210327, USA) and the National Natural Science Foundation of China (nos. 22071102 and 91956110). **Author contributions:** G.L. directed research and wrote the paper. Y.T., Y.W., Q.Y., S.Z., J.-Y.W., S.J., T.X., and J.P. performed and repeated all synthetic experiments and data analysis. K.S. assisted in chiral HPLC analysis. **Competing interests:** The authors declare that they have no competing interests.

Data Availability

All data are available in the manuscript or the Supplementary Materials.

Supplementary Materials

General procedure of asymmetric catalytic AD and Diels–Alder reactions and analytical data, ^{1}H NMR spectra, ^{13}C NMR spectra, and chiral HPLC of resulting products
Fig. S1. ^{1}H NMR Spectra of 1a.
Fig. S2. ^{13}C NMR Spectra of 1a.
Fig. S3. ^{1}H NMR Spectra of 1b.
Fig. S4. ^{13}C NMR Spectra of 1b.
Fig. S5. ^{1}H NMR Spectra of 1c.
Fig. S6. ^{13}C NMR Spectra of 1c.
Fig. S7. ^{1}H NMR Spectra of 1d.
Fig. S8. ^{13}C NMR Spectra of 1d.
Fig. S9. ^{1}H NMR Spectra of 1e.
Fig. S10. ^{13}C NMR Spectra of 1e.
Fig. S11. ^{1}H NMR Spectra of 3a.
Fig. S12. ^{13}C NMR Spectra of 3a.
Fig. S13. ^{1}H NMR Spectra of 3b.
Fig. S14. ^{13}C NMR Spectra of 3b.
Fig. S15. DLS particle size distribution curves of AD-β obtained in THF/Water mixture (5-5 45% H2O, v/v).
Fig. S16. DLS particle size distribution curves of AD-β obtained in THF/Water mixture (1:1 THF: H2O) at times of 30 min, 1 hour, and 2 hours.
Fig. S17. Aggregation-induced catalysis on organocatalytic asymmetric Diels-Alder reaction.
References [*39*–*41*]

References

1. EL Eliel, SH Wilen. *Stereochemistry of organic compounds*. 1st ed. Nashville (TN): John Wiley & Sons; 1994.
2. Jacobsen EN, Pfaltz A, Yamamoto H. *Comprehensive asymmetric catalysis*: *Supplement 1*. 1st ed. Heidelberg (Germany): Springer; 2010.
3. Carreira EM. *Classics in stereoselective synthesis*. 2nd ed. Weinheim (Germany): Wiley-VCH Verlag; 2019.
4. Ojima I. *Catalytic asymmetric synthesis*. 3rd ed. Nashville (TN): John Wiley & Sons; 2013.
5. Corey EJ, Czakó B, Kürti L. *Molecules and medicine*. 1st ed. Hoboken (NJ): Wiley-Blackwell; 2012.
6. Hruby VJ, Li G, Haskell-Luevano C, Shenderovich M. Design of peptides, proteins, and peptidomimetics in chi space. *Biopolymers*. 1997;43(3):219–266.

7. Yudin AK. Macrocycles: Lessons from the distant past, recent developments, and future directions. *Chem Sci*. 2015;6(1):30–49.
8. Taggi AE, Hafez AM, Lectka T. Alpha-imino esters: Versatile substrates for the catalytic, asymmetric synthesis of alpha- and beta-amino acids and beta-lactams. *Acc Chem Res*. 2003;36(1):10–19.
9. Nicolaou KC, Snyder SA. *Classics in total synthesis II more targets, strategies, methods*. 1st ed. Weinheim (Germany): Wiley-VCH Verlag; 2003.
10. Zhang J, Kürti L. Multi-layer 3D chirality: its enantioselective synthesis and aggregation-induced emission. *Natl Sci Rev*. 2021;8(1):Article nwaa205.
11. Bryliakov KP. Chemical mechanisms of prebiotic chirality amplification. *Research (Wash D C)*. 2020;2020:Article 5689246.
12. Bao J, Liu N, Tian H, Wang Q, Cui T, Jiang W, Zhang S, Cao T. Chirality enhancement using Fabry–Pérot-like cavity. *Research (Wash D C)*. 2020;2020:Article 7873581.
13. Zhao T, Han J, Duan P, Liu M. New perspectives to trigger and modulate circularly polarized luminescence of complex and aggregated systems: Energy transfer, photon upconversion, charge transfer, and organic radical. *Acc Chem Res*. 2020;53(7):1279–1279, 1292.
14. Zhao T, Han J, Jin X, Zhou M, Liu Y, Duan P, Liu M. Dual-mode induction of tunable circularly polarized luminescence from chiral metal-organic frameworks. *Research (Wash D C)*. 2020;2020:Article 6452123.
15. Huang G, Wen R, Wang Z, Li BS, Tang BZ. Novel chiral aggregation induced emission molecules: Self-assembly, circularly polarized luminescence and copper(ii) ion detection. *Mater Chem Front*. 2018;2:1884–1892.
16. Li J, Hou C, Huang C, Xu S, Peng X, Qi Q, Lai W-Y, Huang W. Boosting circularly polarized luminescence of organic conjugated systems *via* twisted intramolecular charge transfer. *Research (Wash D C)*. 2020;2020:Article 3839160.
17. Tsuji N, Kennemur JL, Buyck T, Lee S, Prévost S, Kaib PSJ, Bykov D, Farès C, List B. Activation of olefins via asymmetric Brønsted acid catalysis. *Science*. 2018;359(6383):1501–1505.
18. Dhawa U, Tian C, Wdowik T, Oliveira JCA, Hao J, Ackermann L. Enantioselective pallada-electrocatalyzed C-H activation by transient directing groups: Expedient access to helicenes. *Angew Chem Int Ed Engl*. 2020;59(32):13451–13457.
19. Metrano AJ, Chinn AJ, Shugrue CR, Stone EA, Kim B, Miller SJ. Asymmetric catalysis mediated by synthetic peptides, Version 2.0: Expansion of scope and mechanisms. *Chem Rev*. 2020;120(20):11479–11615.
20. Xiong H, Xu H, Liao S, Xie Z, Tang Y. Copper-catalyzed highly enantioselective cyclopentannulation of indoles with donor–acceptor cyclopropanes. *J Am Chem Soc*. 2013;135(21):7851–7854.
21. Chemler SR, Bovino MT. Catalytic aminohalogenation of alkenes and alkynes. *ACS Catal*. 2013;3(6):1076–1091.
22. Dong S, Liu X, Feng X. Asymmetric catalytic rearrangements with α-diazocarbonyl compounds. *Accounts of Chemical Research*. 2022;55:415–428.
23. Ge Y, Qin C, Bai L, Hao J, Liu J, Luan X. A dearomatization/debromination strategy for the [4+1] spiroannulation of bromophenols with α,β-unsaturated imines. *Angew Chem Int Ed Engl*. 2020;59(43):18985–18989.
24. Wang Y-B, Tan B. Construction of axially chiral compounds via asymmetric organocatalysis. *Acc Chem Res*. 2018;51(2):534–547.
25. Wang G, Zhang M, Guan Y, Zhang Y, Hong X, Wei C, Zheng P, Wei D, Fu Z, Chi YR, et al. Desymmetrization of cyclic 1,3-diketones under *N*-heterocyclic carbene organocatalysis: Access to organofluorines with multiple stereogenic centers. *Research (Wash D C)*. 2021;2021:Article 9867915.
26. Cui X, Xu X, Lu H, Zhu S, Wojtas L, Zhang XP. Enantioselective cyclopropenation of alkynes with acceptor/acceptor-substituted diazo reagents via Co(II)-based metalloradical catalysis. *J Am Chem Soc*. 2011;133(10):3304–3307.
27. Liu D, Li B, Chen J, Gridnev ID, Yan D, Zhang W. Ni-catalyzed asymmetric hydrogenation of N-aryl imino esters for the efficient synthesis of chiral α-aryl glycines. *Nat Commun*. 2020;11(1):5935.
28. Rouh H, Tang Y, Xu T, Yuan Q, Zhang S, Wang J-Y, Jin S, Wang Y, Pan J, Wood HL, et al. Aggregation-Induced Synthesis (AIS): Asymmetric Synthesis via Chiral Aggregates. *Research (Wash D C)*. 2022;2022:Article 9865108.
29. Wu G, Liu Y, Yang Z, Katakam N, Rouh H, Ahmed S, Unruh D, Surowiec K, Li G. Multilayer 3D chirality and its synthetic assembly. *Research (Wash D C)*. 2019;2019:Article 6717104.
30. Liu Y, Wu G, Yang Z, Rouh H, Katakam N, Ahmed S, Unruh D, Cui Z, Lischka H, Li G. Multi-layer 3D chirality: New synthesis, AIE and computational studies. *Sci China Chem*. 2020;63:692–698.
31. Hu M, Feng H-T, Yuan Y-X, Zheng Y-S, Tang BZ. Chiral AIEgens – Chiral recognition, CPL materials and other chiral applications. *Coord Chem Rev*. 2020;416:Article 213329.
32. Xu H, Liu L, Teng F, Lu N. Emission enhancement of fluorescent molecules by antireflective arrays. *Research (Wash D C)*. 2019;2019:Article 3495841.
33. Wu G, Liu Y, Yang Z, Ma L, Tang Y, Zhao X, Rouh H, Zheng Q, Zhou P, Wang J-Y, et al. Triple-columned and multiple-layered 3D polymers: Design, synthesis, aggregation-induced emission (AIE), and computational study. *Research (Wash D C)*. 2021;2021:Aricle 3565791.
34. Tang Y, Zhang S, Xu T, Yuan Q, Wang J-Y, Jin S, Wang Y, Pan J, Griffin I, Chen D, et al. Aggregation-induced polarization (AIP): Optical rotation amplification and adjustment of chiral aggregates of folding oligomers and polymers. *Front Chem*. 2022;10:Article 962638.
35. Tang Y, Yuan Q, Wang Y, Zhang S, Wang J-Y, Jin S, Xu T, Pan J, Guilbeau CR, Pleasant AJ, et al. Aggregation-induced polarization (AIP) of derivatives of BINOL and BINAP. *RSC Adv*. 2022;12(46):29813–29817.
36. Kolb HC, VanNieuwenhze MS, Sharpless KB. Catalytic asymmetric dihydroxylation. *Chem Rev*. 1994;94(8):2483–2547.
37. Berrisford DJ, Bolm C, Sharpless KB. Ligand-accelerated catalysis. *Angew Chem Int ed Engl*. 1995;34(10):1059–1070.
38. Sharpless KB, Amberg W, Beller M, Chen H, Hartung J, Kawanami Y, Lubben D, Manoury E, Ogino Y, Shibata T, et al. New ligands double the scope of the catalytic asymmetric dihydroxylation of olefins. *J Org Chem*. 1991;56(15):4585–4588.
39. Ahrendt KA, Borths CJ, MacMillan DWC. New strategies for organic catalysis: The first highly enantioselective organocatalytic Diels−Alder reaction. *J Am Chem Soc*. 2000;122(17):4243–4244.
40. Brochu MP, Brown SP, MacMillan DWC. Direct and enantioselective organocatalytic α-chlorination of aldehydes. *J Am Chem Soc*. 2004;126(13):4108–4109.
41. Wilson RM, Jen WS, Macmillan DWC. Enantioselective organocatalytic intramolecular Diels-Alder reactions. the asymmetric synthesis of solanapyrone D. *J Am Chem Soc*. 2005;127(33):11616–11618.